Catal Lett (2009) 128:313–317
DOI 10.1007/s10562-008-9757-1

A Possible Mechanism of Hydrogen Reverse Spillover in Platinum-Zeolite Catalysts

M. N. Mikhailov · I. V. Mishin · L. M. Kustov

Received: 23 September 2008 / Accepted: 27 October 2008 / Published online: 13 November 2008

Abstract Quantum chemical methods (X3LYP and MP2) were applied to investigate the structure and reactivity of anion-radical site in HZSM-5 zeolite. The interaction of hydrogen zeolite with a platinum particle can involve electron transfer to a Brønsted acid site to form an anion-radical fragment. A low stability of the latter favors the elimination of atomic hydrogen from the OH-group, an exothermic process with low activation energy. In the metal-zeolite catalysts, the anion-radical fragment formed due to withdrawal of electronic density from the metal particle can be responsible for the reverse spillover of Brønsted hydrogen onto the metal surface.

Keywords Brønsted acid site · Electron transfer · Anion-radical site · Hydrogen elimination

1 Introduction

Platinum containing zeolites are important catalysts for hydrocarbon transformations. Conventional description of bifunctional Pt/zeolite catalysts implies the independent functioning of metal and acid sites [1, 2]. According to this concept, hydrogenation and dehydrogenation occur on a metal particle, whereas C–C bond activation proceeds on an acid site. This picture suggests two different kinds of sites and a negligible mutual influence among metal and acid sites [3]. However, Bremer and Minachev were among the first who indicated a catalytic significance of the interaction between metal particles and OH-groups in platinum containing zeolites [4, 5]. They found that the hydrogen spillover on catalyst surface occurs at ambient temperatures. Moreover, we have showed that the introduction of the Pt_6 cluster in the HZSM-5 zeolite channel results in withdrawal of electronic density from the platinum, particle to Brønsted acid site (BAS) and hydrogen transfer from the hydroxyl onto the metal surface (reverse hydrogen spillover) [6–9]. The process can be interpreted as due to the formation of the $[Pt_6H]^+$ complex cation in a cationic position with the hydrogen presenting in the form of an adsorbed hydrogen atom. This in turn leads to oxidation of the metal particle and suppression of Brønsted acidity of the zeolite support. It is known that the values of BAS deprotonation energies are very high, ranging from 280 to 320 kcal/mol [10–13]. These values are difficult to reconcile with the fact that the reverse hydrogen spillover is of an exothermic nature, and it proceeds with negligible low activation energy. Accordingly, it seems of interest to perform a quantum-chemical study of the structure and reactivity of an electron-enriched zeolite fragment (anion-radical site) formed upon the electron density transfer to BAS in high-silica zeolites.

2 Computational Details

To model the fragment of zeolite, the cluster approach was used. The cluster electronic structure was computed using the X3LYP density functional method [14] as well as second order Møller-Plesset perturbation theory (MP2). The DFT method was used unless otherwise stated. The 6-31+G(d,p) basis set was used. Calculations were

This paper is dedicated to the memory of Professor Heinrich Bremer (1920–2008).

M. N. Mikhailov (✉) · I. V. Mishin · L. M. Kustov
N.D. Zelinsky Institute of Organic Chemistry, Russian Academy of Sciences, Russian Federation, Leninsky Prospect 47, 119991 Moscow, Russia
e-mail: mik@ioc.ac.ru

performed with the PC GAMESS program package [15, 16]. Cluster modeling the fragment of ZSM-5 zeolite framework was constructed by coupling three-five-member rings, located at the intersection of straight and sinusoidal channels, and it includes 10 silicon atoms and one aluminum atom (T_6 position). The cluster broken Si–O bonds were saturated with hydrogen atoms, placed at 1.5 Å along Si–O bonds. All terminal hydrogen atoms were fixed during the geometry optimization. A proton of BAS compensated for the excessive negative charge of the framework. The cluster obtained has the $AlSi_{10}O_{12}H_{18}(OH)$ stoichiometry, and it further is denoted as ZOH.

3 Results and Discussion

Figure 1 shows the cluster modeling zeolite fragment. The BAS is represented by a bridged hydroxyl group O1H1, located between Al1 and Si1 atoms at the intersection of three-five-member rings in a straight channel of ZSM-5 zeolite. Table 1 lists geometric parameters and charges for the BAS (ZOH) as well as for the anion-radical (ZOH^{*-}) and anion (ZO^{-}) zeolite fragments. The geometric parameters for ZOH and ZO^{-} are in agreement with published data [17, 18]. In ZOH, the Al1–O1 distance is 0.22 Å higher than that of Si1–O1. The electron configuration for the hydrogen atom in the bridged hydroxyl group is $1\ s^{0.43}$.

There are two possible pathways of the bridged hydroxyl group dissociation. The heterolytic cleavage (1) of O1–H1 bond leads to a proton (H^{+}) elimination, whereas the homolytic rupture (2) results in an atomic hydrogen (H^{*}) abstraction:

$$ZOH \rightarrow ZO^{-} + H^{+} \quad \Delta E = 284\,\text{kcal/mol} \tag{1}$$

$$ZOH \rightarrow ZO^{*} + H^{*} \quad \Delta E = 109\,\text{kcal/mol} \tag{2}$$

Since the energy of reaction (2) is much lower than that of reaction (1), the suggestion is plausible that the anion-radical fragment ZOH^{*-} (Table 1), produced when an electron is captured by BAS, will be characterized by a more favorable H^{*} elimination. Calculations of the energies for the heterolytic (3) and homolytic (4) processes for OH-group dissociation in the anion-radical ZOH^{*-} gave the following results:

$$ZOH^{*-} \rightarrow ZO^{*2-} + H^{+} \quad \Delta E = 356\,\text{kcal/mol} \tag{3}$$

$$ZOH^{*-} \rightarrow ZO^{-} + H^{*} \quad \Delta E = -21\,\text{kcal/mol} \tag{4}$$

The homolytic cleavage (4) of the O1–H1 bond becomes thermodynamically favorable. The formation of an anion-radical site induced by the electron transfer from an adsorbed donor molecule (platinum particle) to electron-acceptor site of zeolite (BAS) appears to be possible if the chemical potentials of the donor molecule (μ_d) and electron-acceptor zeolite fragment (μ_a) meet the following condition:

$$\Delta\mu = \mu_a - \mu_d = \left(\frac{\partial E_a}{\partial N}\right)_v - \left(\frac{\partial E_d}{\partial N}\right)_v = \frac{IE_d + EA_d}{2} - \frac{IE_a + EA_a}{2} < 0, \tag{5}$$

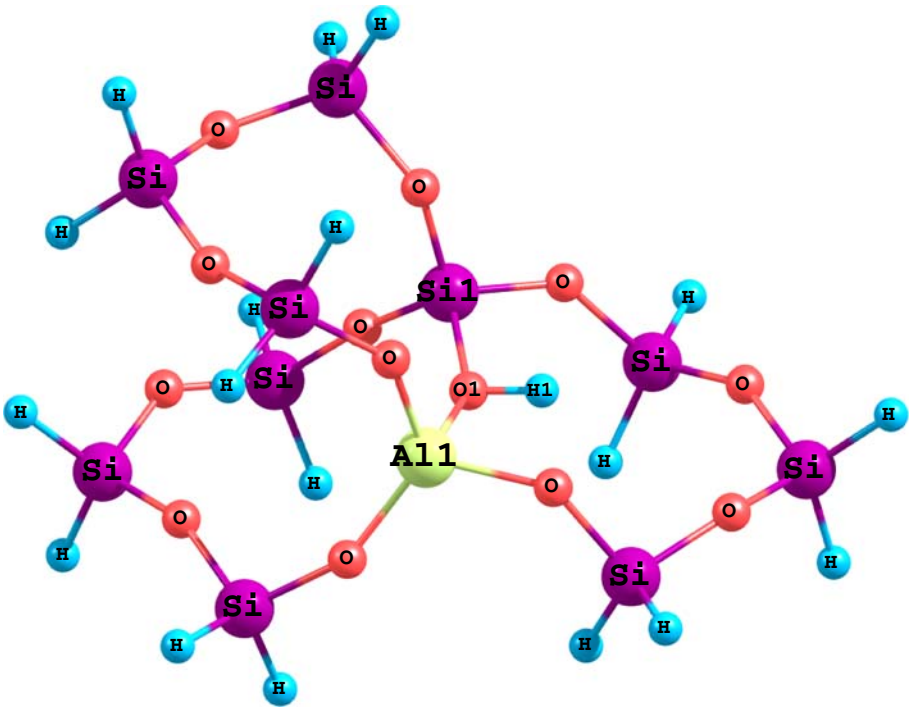

Fig. 1 Cluster modeling HZSM-5 zeolite fragment

Table 1 Bond lengths and natural charges (q) in different zeolite fragments

Structure	Bond length, Å			q(Al1)	q(Si1)	q(O1)	q(H1)
	Al1–O1	Si1–O1	H1–O1				
ZOH	1.92	1.70	0.98	2.16	2.58	−1.18	0.57
ZOH^{*-}	1.83	1.84	0.98	2.14 (0.02)	2.00 (0.69)	−1.21 (0.05)	0.54 (0.04)
ZO^{-}	1.75	1.59	–	2.14	2.56	−1.36	–

Natural spin densities are given in brackets

where μ is the chemical potential, E is the electron energy of a system, N is the number of electrons, IE is the ionization energy, EA is the electron affinity, v is the external potential, while subscripts a and d stand for the acceptor and donor molecules, respectively.

Table 2 contains the values of IE, EA, μ, and $\Delta\mu$ calculated for the Pt_6 particle adsorbed in the channel of HZSM-5 zeolite [9] and zeolite fragment ZOH. The data indicate that platinum particle is characterized by the values of $\Delta\mu < 0$ supporting the feasibility of anion-radical site formation upon electron transfer to BAS. With the electron capture, the Al1–O1 bond shortens, whereas the Si1–O1 bond lengthens, equalizing lengths of the bonds. The bond length in the hydroxyl group and the electron configuration of the hydrogen atom remain practically unchanged. The spin density of an unpaired electron is essentially localized on silicon atom Si1. As the anion-radical forms, the charge on Si1 atom decreases by 0.58 (Table 1). To throw some light onto the magnitude of the activation energy of a homolytic dissociation of O1–H1 bond in anion-radical ZOH^{*-}, the potential energy surface (PES) scans as a function of O1–H1 distance were calculated (Fig. 2) at the X3LYP (D) and MP2 (D′) levels. During the calculations, O1–H1 bond length was fixed, and geometry was fully optimized except for the positions of terminal hydrogen atoms. The shape of the PES for the ground doublet state D is a result of an avoided crossing of D_1 and D_2 terms corresponding to the $ZO^{-}H^{*}$ and $ZO^{*2-}H^{+}$ systems, respectively. It is known that an adiabatic approach cannot be used to treat the intersection between two electronic states. The nonadiabatic region is indicated by the circle in Fig. 2. Since the intersection occurs in the local region of reaction coordinate, the

Table 2 Vertical ionization energies (IE), electron affinities (EA), and chemical potentials (μ) for the donor molecules and zeolite fragment

Structure	IE, eV	EA, eV	μ, eV	$\Delta\mu$, eV
Pt_6[9][a]	4.9	1.1	−3.0	−1.5
ZOH	9.4 (9.2)	−0.4 (0.3)	−4.5 (−4.7)	

[a] Pt_6 particle adsorbed in the channel of HZSM–5 zeolite

Adiabatic values are given in brackets

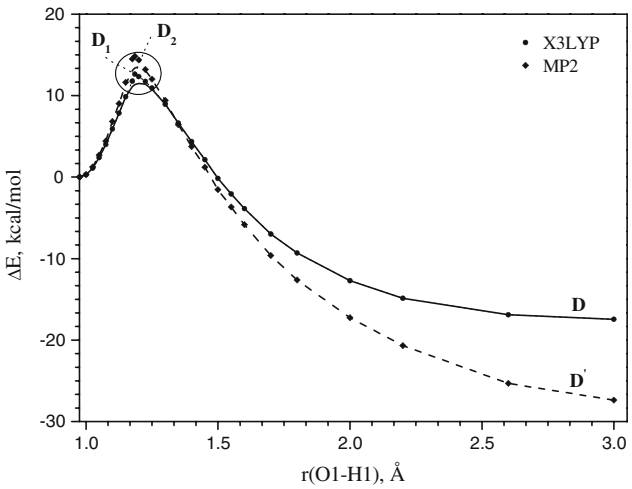

Fig. 2 Potential energy scan along O1–H1 distance for the anion-radical fragment in HZSM-5 zeolite

nonadiabatic region can be satisfactorily approximated by the pair of hyperbolas with the asymptotes defined as the tangent lines to the curves of D_1 and D_2 potential surfaces. Therefore the intramolecular electron transfer can be described with the help of PES (D), constructed by combining the PES of states before (D_2) and after (D_1) electron

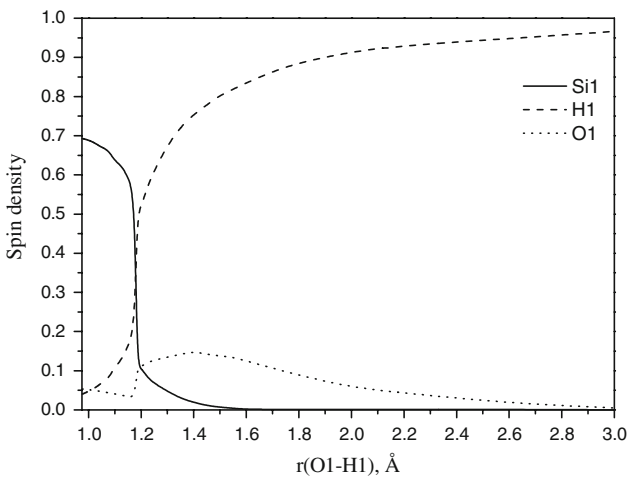

Fig. 3 Natural spin density on Si1, H1, and O1 atoms as a function of the O1–H1 distance

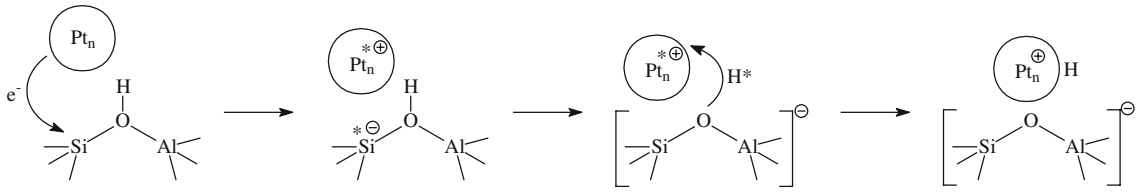

Fig. 4 Scheme of the anion-radical site formation upon interaction of BAS with a platinum particle and subsequent reverse spillover of hydrogen

transfer. In the process of intramolecular electron transfer, the D_1 and D_2 states become isoenergetic (r(O1H1) = 1.19 Å) while the PES scan along the O1–H1 bond length in the ground state (D) is characterized by a barrier as high as 12 kcal/mol. The MP2 method (D′ curve) predicts nearly the same activation energy as the X3LYP method does but with somewhat higher stability for the $ZO^- + H^*$ system (~10 kcal/mol).

Figure 3 shows the natural spin density on Si1, H1 and O1 atoms as a function of the O1–H1 distance. As the O1–H1 distance increases, intramolecular electron transfer is observed from the Si1 silicon atom to the H1 hydrogen atom. Spin density decreases on the silicon atom and increases on the hydrogen atom. In the pre-barrier region (r(O1H1) < 1.19 Å), spin density is substantially localized on silicon atom. After passing the barrier at r(O1H1) = 1.19 Å, the spin density of the unpaired electron mainly shifts to the hydrogen atom, and the Brønsted proton acquires the properties of the atomic hydrogen. In the pre-barrier region, the spin density on the oxygen atom of the hydroxyl group remains practically unchanged. In the post-barrier region, it reaches a maximum (0.15) at r(O1H1) = 1.4 Å and then approaches zero. When the O–H bond length reaches a value of 3.0 Å, a nearly full electron transfer occurs from the Si1 silicon atom to the H1 hydrogen atom, and leads to the formation of a ZO^- anion fragment of zeolite (Table 1) and atomic hydrogen. Hydrogen abstraction from the hydroxyl group is accompanied by the increase in charge on the Si1 silicon atom by 0.56 and the decrease in charge on O1 oxygen atom by 0.15; the charge on the H1 hydrogen atom decreases from 0.54 to 0.0. The charge (~2.14) and spin density (~0.04) on the Al1 atom remain practically unchanged. In the process of atomic hydrogen elimination, the cluster's band gap decreases from 2.8 eV for the initial anion-radical fragment (r(O1H1) = 0.98 Å) to 1.4 eV for the barrier region (r(O1H1) = 1.19 Å) and then increases up to 5.8 eV for the $ZO^- + H^*$ system (r(O1H1) = 3.0 Å).

The mechanism of atomic hydrogen elimination upon an anion-radical fragment formation in zeolite is ready for use in the explanation of the metal–acid site interaction in bifunctional catalysts. A possible mechanism (Fig. 4) governing the proton transfer involves withdrawal of electronic density from the platinum particle onto BAS to generate an anion-radical fragment in the zeolite framework. The second step includes an O–H bond cleavage and the elimination of a hydrogen atom followed by adsorption on the platinum surface. In the presence of platinum particle the activation energy of hydrogen atom elimination drastically reduces and the reaction energy (ΔE) for the reverse spillover attains the value of –40 kcal/mol [6, 7]. The mechanism of hydrogen transfer upon electron capture may be operative when alkenes and aromatics interact with electron-acceptor sites of high-silica zeolites to form corresponding cation-radicals [19, 20].

4 Conclusion

Thus, the interaction of the hydrogen form of zeolite with adsorbed platinum particle can lead to the electron transfer from the metal cluster to BAS to form an anion-radical fragment. The anion-radical fragment formed is unstable, and it experiences atomic hydrogen elimination with low activation energy. In the metal-zeolite catalysts, the anion-radical fragment formed due to withdrawal of electronic density from the metal particle onto BAS can be responsible for the reverse spillover of BAS hydrogen atom onto the metal surface and the formation of a stabilized metal cluster in an oxidized state.

Acknowledgments The authors gratefully acknowledge the critical reading of the manuscript by Dr. Walter H. Niehoff.

References

1. Weisz PB, Swegler EW (1957) Science 126:31
2. Kuhlmann A, Rössner F, Schwieger W, Gravenhorst O, Selvam T (2004) Catal Today 97:303
3. Ono Y (2003) Catal Today 81:3
4. Steinberg K-H, Hofmann F, Bremer H, Dmitriev RV, Detjuk AN, Minachev KhM (1979) Z Chem 19:34
5. Minachev KhM, Dmitriev RV, Detyuk AN, Steinberg K-H, Bremer H (1978) Bull Acad Sci USSR Div Chem Sci 27:2394
6. Mikhailov MN, Kustov LM, Kazansky VB (2008) Catal Lett 120:8
7. Mikhailov MN, Mishin IV, Kustov LM, Microporous Mesoporous Mater. doi 10.1016/j.micromeso.2008.08.014
8. Mikhailov MN, Mishin IV, Kustov LM, Mordkovich VZ (2009) Catal Today (in press)

9. Mikhailov MN, Kustov LM, Mordkovich VZ, Stakheev AYu (2008) Russ Chem Bull 57 (in press)
10. Kramer GJ, van Santen RA (1993) J Am Chem Soc 115:2887
11. Brand HV, Curtiss LA, Iton LE (1993) J Phys Chem 97:12773
12. Brand HV, Curtiss LA, Iton LE (1992) J Phys Chem 96:7725
13. Redondo A, Hay PJ (1993) J Phys Chem 97:11754
14. Xu X, Zhang Q, Muller RP, Goddard WAIII (2005) J Chem Phys 122:014105
15. Schmidt MW, Baldridge KK, Boatz JA et al (1993) J Comput Chem 14:1347
16. Granovsky AA, PC GAMESS version 7.1. http://classic.chem.msu.su/gran/gamess/index.html
17. Yuan SP, Wang JG, Li YW, Jiao H (2002) J Phys Chem A 106:8167
18. Barone G, Casella G, Giuffrida S, Duca D (2007) J Phys Chem C 111:13033
19. Slinkin AA, Kucherov AV, Kondratyev DA, Bondarenko TN, Rubinstein AM, Minachev KhM (1986) J Mol Catal 35:97
20. Kucherov AV, Slinkin AA, Kondratyev DA, Bondarenko TN, Rubinstein AM, Minachev KhM (1986) J Mol Catal 37:107